Journal of the Air Pollution Control Association

ISSN: 0002-2470 (Print) (Online) Journal homepage: https://www.tandfonline.com/loi/uawm16

Lidar Applications in Air Pollution Research and Control

Warren B. Johnson

To cite this article: Warren B. Johnson (1969) Lidar Applications in Air Pollution Research and Control, Journal of the Air Pollution Control Association, 19:3, 176-180, DOI: 10.1080/00022470.1969.10466474

To link to this article: https://doi.org/10.1080/00022470.1969.10466474

Warren B. Johnson
Stanford Research Institute

Lidar Applications In Air Pollution Research and Control

The fundamental capabilities and limitations of the lidar (laser radar) in observing particulate concentrations in the atmosphere are discussed. The advantages of the lidar technique stem from its ability to obtain measurements remotely and at a high density in space and time. The quantitative application of the technique is limited by the accuracies with which: (1) the separate effects upon the return signal of backscatter and attenuation may be identified; and (2) the optical parameters may be related to the characteristics of the aerosol. The main areas of utility for lidar in air pollution research and control are: (1) to observe the structure and height of mixing layers; (2) to measure the transport and diffusion of plumes or clouds of particulates; and (3) to remotely determine smoke-plume opacity. These applications are briefly reviewed and exemplified.

Since its development for meteorological use in 1963 by the late M. G. H. Ligda and his co-workers at Stanford Research Institute, the lidar (or laser radar) has proved to be an instrument of great value in a wide variety of atmospheric studies. Its utility in air-pollution investigations stems from its ability to remotely detect particulate matter in the atmosphere at ranges up to 10 km or more. Being an active system, the lidar draws added advantage from being independent of external sources of electromagnetic radiation. The purpose of this paper is to review the main areas in which this instrument can be of use in air pollution research and control: (1) to observe the structure and height of surface-based mixing layers; (2) to measure the transport and diffusion of plumes and clouds of particulates; and (3) to remotely determine smoke-plume opacity.

Only a brief discussion regarding the characteristics of a lidar and its signal return will be presented here; additional information is contained in the papers by Ligda (1965)[1], Collis (1966)[2], Barrett and Ben-Dov (1967)[3], and Northend, *et al.* (1966)[4].

One of the more versatile of the SRI lidars is the Mark V, pictured in Figure 1. The characteristics of this instrument are described in the Appendix. As with all lidars, the Mark V is basically composed of a laser transmitter, which emits a very brief, high-intensity pulse of coherent light, and a receiver, which detects the energy at that wavelength backscattered from the atmospheric aerosol as a function of range. The lidar equation contains two related unknowns, the backscattering and attenuation coefficients, which have separate and opposing effects upon the magnitude of the signal return. Under certain conditions, such as when the attenuation is negligible, or when the backscatter is approximately constant in a homogeneous atmosphere, the two coefficients can be easily evaluated as a function of range, which is the prime information to be gained from a lidar observation. At other times it is necessary to assume the form of the relationship between the backscatter and attenuation; this is the approach taken by Barrett and Ben-Dov (1967)[3]. The lidar technique for measuring particulate concentrations is an indirect one, in that only optical parameters are obtained, which must then be related to the amount of material present.

The prime contribution to the attenuation at wavelengths close to that of the ruby lidar (0.694μ), for a shot in the "clear" lower atmosphere, is from Mie scattering by particulate matter. Under these conditions, Elterman's (1964)[5] model of a clear standard atmosphere predicts that less than four percent error is introduced if the attenuation due to Rayleigh scattering and ozone absorption is neglected. Figure 2 compares typical lidar wavelengths with the sizes of common atmospheric particles. Mie scattering is normally considered to prevail when the particles are larger than about 1/10 of the wavelength. Thus, at the ruby-lidar wavelength, Mie scattering occurs from particles larger than about 0.07μ in diameter, which, as shown in the figure, includes a large portion of the smoke and haze particles normally present in polluted atmospheres.

The backscattering coefficient is a function of the number concentration, size distribution, and optical properties of the particulates. If the size distribution and optical properties are measured or assumed, the absolute aerosol mass concentration can be evaluated from a lidar return. Accurate information of this sort, however, is not normally available. Frequently, though, the aerosol *size* distribution and optical properties can be assumed to be stable and reasonably uniform in space (McCormick and Kurfis, 1966)[6]. Using

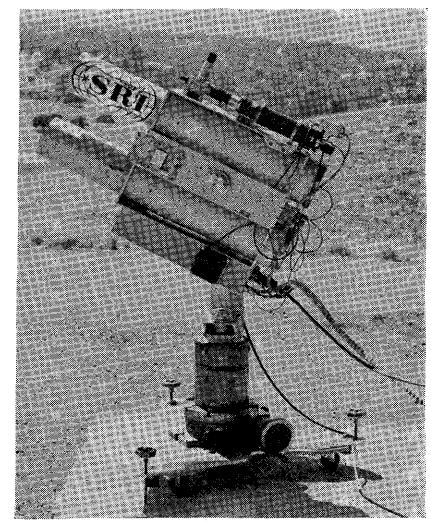

Figure 1. Stanford Research Institute Mark V Lidar.

Dr. Johnson is Senior Research Meteorologist in the Aerophysics Laboratory, Stanford Research Institute, Menlo Park, California.

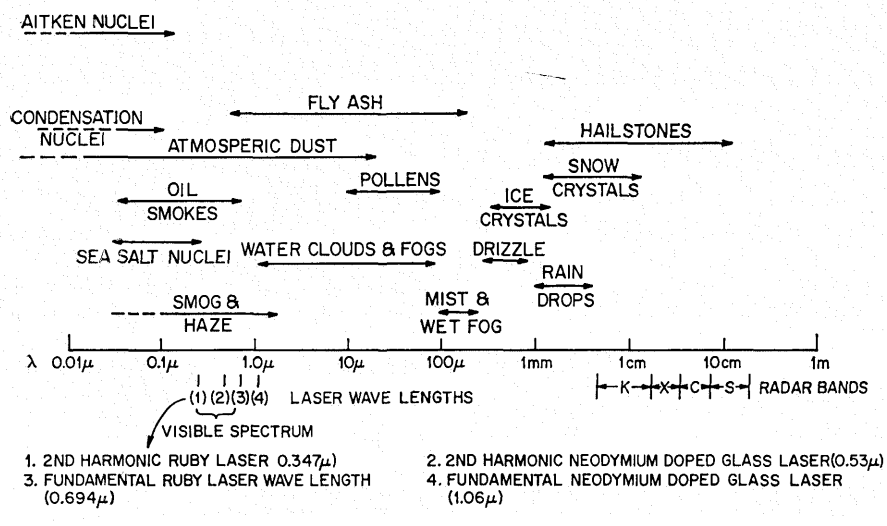

Figure 2. Relation of typical lidar wavelengths to diameters of common atmospheric particles.

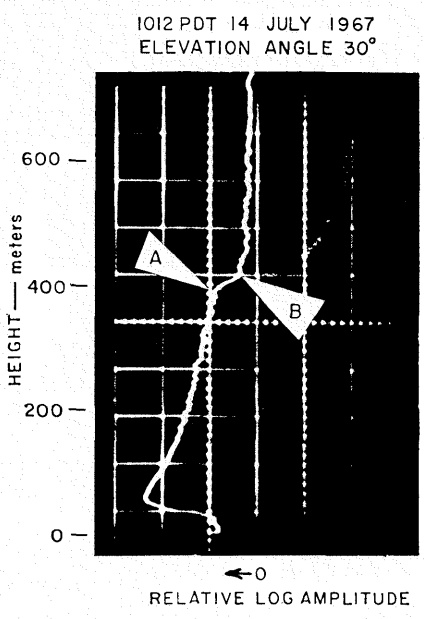

Figure 3. Sample lidar return showing the transition from relatively polluted air below the inversion base to cleaner air above.

this assumption, at any point the backscattering coefficient measured by the lidar is directly proportional to the particulate mass concentration. Such information, when combined with backscatter measurements from the "background" clean air frequently found upwind of or above a polluted area or layer, often can be used to map the spatial distribution of particulate matter in terms of *relative* concentrations, which give the contributions due to the added pollutants. If the actual particle size distribution is measured by independent means or a reasonable estimate may be made, however, the use of the Mie scattering theory permits the calculation of absolute concentrations from the lidar data, after the effects of backscatter and attenuation are separated.

Lidar Observations of the Structure and Height of Mixing Layers

Vertical changes in the atmospheric thermal stability, particularly temperature inversions, are almost invariably reflected in the vertical aerosol structure. When the source of particulate pollution is beneath an inversion, the upward mixing of the pollution is limited by the base or some slightly higher level of the inversion. If the source is within a stable layer, possibly above an inversion base as in the case of a tall stack, the particulates tend to spread out in a horizontal sheet with little vertical diffusion.

An upward-directed lidar shot can give a very accurate measurement of the height of the mixing layer, an important parameter in estimating the dilution capacity of the atmosphere. In addition, the relative concentration distribution of particulates within the mixing layer may be obtained. A typical lidar return illustrating this effect is shown in Figure 3. The "artificial" peak signal at about 75-m height is the approximate point at which the transmitter beam and receiver field of view initially intersect. (Current lidars have separate transmitter and receiver optics. The fabrication of a truly coaxial instrument must await the development of a suitable optical equivalent of the radar transmit/receive switch.) Above the 75-m level the signal decreases steadily approximately as range^{-2}, indicating a relatively homogeneous aerosol up to Point *A*, which marks the base of a temperature inversion. At this level, the signal begins to decrease rapidly to a value at Point B indicative of much cleaner air.

Time series of such observations have shown some interesting variations in the height of the aerosol discontinuity. Hamilton (1966a)[7] observed height changes between 900 and 1200 m over a 20-min period, which were apparently due to rising convective bubbles impinging upon the inversion. The series of observations shown in Figure 4, from Viezee and Oblanas (1969),[8] illustrates the growth of the mixing layer (as indicated by the depth of the primary haze layer) with increasing surface heating, convection, and subsequent lifting of the temperature inversion. On this occasion the lidar also observed a weak aerosol concentration above the inversion, possibly the result of penetrative convection. The temperature profiles concurrently obtained extended only up to 800 m, hence the association of the apparent secondary haze boundary with a second, upper inversion may only be speculated upon.

The detection of inversion layers by lidar is not necessarily dependent upon

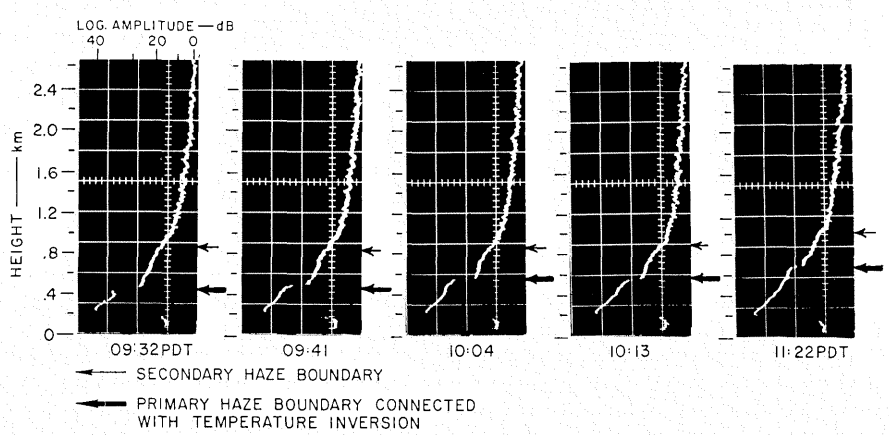

Figure 4. Oscilloscope photographs of the vertical profiles of received signal power versus height recorded with Mark V ruby lidar at Menlo Park, California, 26 August 1968 (lidar elevation angle, 70°).

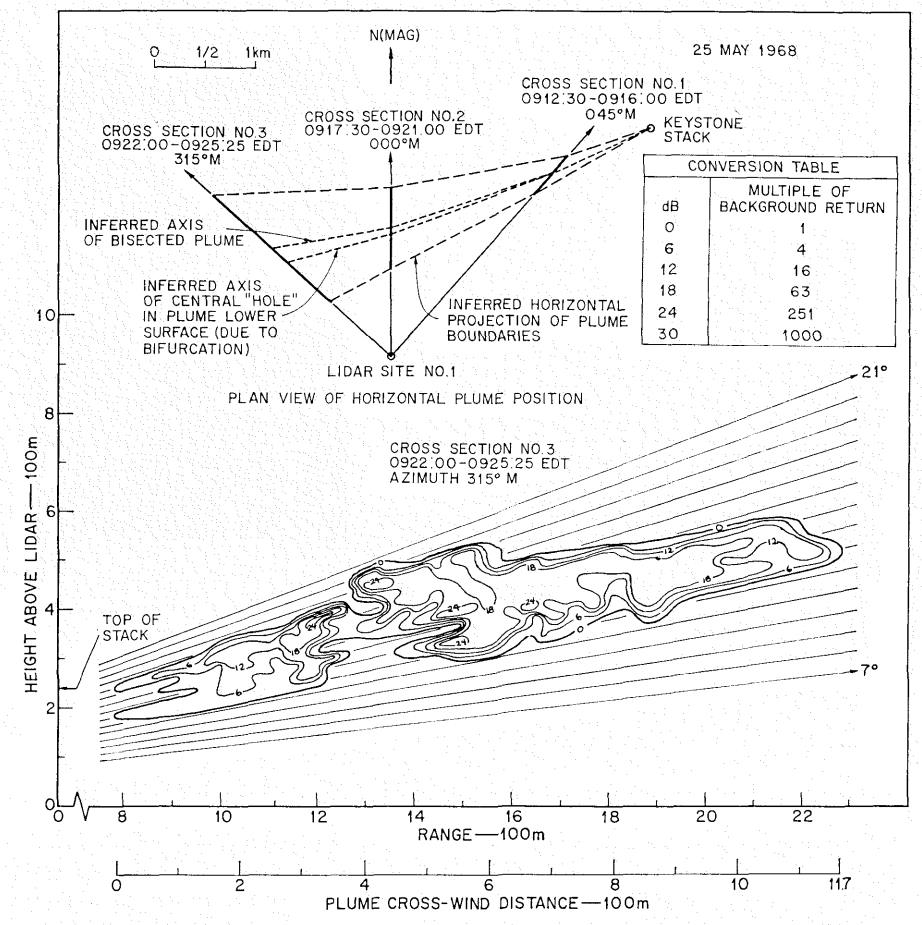

Figure 5. Typical vertical cross-section through the smoke plume from the 800-ft stack of a large coal-fired power plant, observed by lidar under stable conditions. The contours represent range-corrected signal in dB relative to that from the ambient (background) aerosol, including background noise, and can be taken to represent relative particulate concentrations. Attenuation has been neglected. See inset for horizontal positions of cross sections. The "hole" in the bottom of the plume was present in all three cross sections at the different downwind distances, and is apparently the manifestation of plume bifurcation.

man-made pollution. Observations in apparently clear rural atmospheres indicate that sufficient naturally-occurring aerosols are frequently present to enable useful deductions of thermal structure to be made. Lidar is so well suited for the monitoring of the vertical structure of mixing layers that it seems reasonable to expect their routine use on an operational basis at major cities in the future.

Measurement of the Transport and Diffusion of Plumes and Clouds of Particulates

The tenuous nature of the plumes from most modern power plants makes the study of the diffusion of such plumes by photographic techniques impractical. The problems associated with using networks of fixed samplers to furnish information about plume behavior also are well known to the air pollution meteorologist. The usefulness of lidar in furnishing detailed, three-dimensional relative concentration distributions of plumes or clouds containing particulate material is becoming increasingly apparent. Lidar has been used successfully to study plume rise and diffusion from power plant stacks (Johnson, 1969[9]; Hamilton, 1966b[10], 1967[11]), to investigate the diffusion characteristics of insecticide spray plumes released by aircraft (Collis, 1968[12]), and to document the movement and spread of dust clouds from explosions (Oblanas and Collis, 1967)[13].

An example of the results of the lidar observations of the smoke plume from a large coal-burning power plant, from Johnson (1969)[9], is presented in Figure 5. The vertical cross section was obtained from sequential lidar shots at 1° elevation increments. The contours represent the range-corrected amplitude of signal return (in logarithmic units) relative to that from the background, and as such can be taken to be approximately proportional to smoke concentrations, if the particle size distribution is assumed to be spatially uniform and the slight amount of attenuation is neglected. The plan view in the figure illustrates the operational technique used in the field, in which the mobile lidar was located a few kilometers from the plume centerline, and then a series of several vertical cross sections at different azimuth angles were obtained. These successive cross sections at increasing downwind distances reveal the rise, diffusion, and changes in structure of the plume in response to the meteorological influences present.

In this example, the horizontal "fanning" and tilt of the plume caused by vertical wind direction shear under stable conditions is apparent. Other observations showed diffusion under fumigation and looping conditions, and influences due to terrain features. Strong lidar returns from the smoke plume from this stack have been obtained under stable conditions as far as 13 miles downwind from the source.

Remote Determination of Smoke-Plume Opacity

A recent feasibility study by W. E. Evans of Stanford Research Institute has indicated that lidar can be successfully used as a single-ended transmissometer to furnish objective, repeatable measurements of the opacity of smoke plumes from industrial stacks. The principle involved in this technique is illustrated in Figure 6. A lidar shot is made through the plume, and the two-way attenuation of the laser energy by the plume is measured. In Figure 6(a), a portion of the signal return from such a lidar shot is shown. (In this presentation, no correction has been made for the normal decrease in return due to atmospheric attenuation and increasing range.) Where the pulse hits the plume at 400 m, there is a large backscattered signal that is not utilized in the present technique. (In actual practice this return spike must be gated out to prevent photomultiplier tube saturation and ringing.) The dashed line indicates the return to be expected for a shot in the "clear" air to the side of the plume. The amount of the offset of the waveform, or the ratio of the signal level received due to the backscatter from the air behind the plume to that which would be received in the absence of the effluent determines the transmission of the plume. Figure 6(b) indicates how the amount of this offset varies with increasing plume opacities (decreasing transmissions). In an actual operating system, more sophisticated data-display techniques would facilitate the measurement of the offset.

Field tests have been carried out of the capability of the ruby-lidar technique in measuring the transmission of a variety of test targets and also of an oil-fired smoke plume. Comparative transmission measurements were made using

the conventional two-ended technique, employing a tungsten light source filtered to a narrow band about the ruby wavelength. Lidar measurements made on the test targets were in good agreement with the readings of the conventional instruments. Tests on the smoke plume, which was extremely tenuous, resulted in a lidar signal attenuation which was so small as to be unmeasurable with the data-display method used. It was concluded that an improved display/analysis technique is needed to obtain accurate measurements of plumes having transmissions greater than about 90 percent.

In a mobile system, this instrument appears to have great promise in air pollution control and enforcement, and should furnish a much firmer basis for the determination of smoke-plume acceptability than presently-used subjective techniques such as the Ringelman test. In this regard, concurrent use of a lidar and an infrared interference spectrometer, such as that described by Low (1967)[14], could make possible the monitoring of both particulate and gaseous products in stack plumes.

The capability of lidar as a single-ended transmissometer could also be used to advantage in air pollution studies for the convenient and objective measurement of horizontal and slant visibilities in smog.

Concluding Remarks

All of the applications which have been discussed in this paper depend upon the ability of lidar to detect particulate material in the atmosphere. A further possibility, which is currently under study, is the detection of certain gases by the differences in their absorption of the different wavelengths of two lidars.

It seems clear that lidar appears destined to assume an increasingly important role in air pollution research and control, in addition to its other applications in areas such as ceilometry and cloud physics. The present capability of lidar to obtain data of a high density in time and space, particularly in the important vertical dimension, is unmatched. Present equipment limitations with regard to pulse repetition frequency and data-handling rates are largely economic and can be readily removed using current technology. Someday, radar-type displays should give air-pollution workers as complete a picture of particulate distributions as meteorologists now have of storm patterns.

Acknowledgments

I am grateful to Mr. William Evans of Stanford Research Institute for allowing me to describe his unpublished research on the use of lidar to determine smoke-plume opacity. This review has also drawn upon the work of several other of my associates at the Institute: Mr. Ronald Collis, Dr. Edward Uthe, Mr. William Viezee, Mr. John Oblanas, and Mr. Fred Fernald (now at the University of Arizona). Portions of the research described were supported by the National Air Pollution Control Administration (Meteorology Program), the Edison Electric Institute, and the Air Force Cambridge Research Laboratories.

References

1. Ligda, M. G. H., "The laser in meteorology," *Discovery*, **26**, 30–35 (1965).
2. Collis, R. T. H., "Lidar: a new atmospheric probe," *Quart. J. Roy Meteor. Soc.*, **92**, 220–230 (1966).
3. Barrett, E. E., and Ben-Dov, O., "Applications of the lidar to air pollution measurements," *J. Appl. Meteor.*, **6**, 500–515 (1967).
4. Northend, C. A., Honey, R. C., and Evans, W. E., "Laser radar (lidar) for meteorological observations," *Rev. Scient. Instr.*, **37**, 393–400 (1966).
5. Elterman, L. "Atmospheric attenuation model, 1964, in the ultraviolet, visible, and infrared regions for altitudes to 50 km," Environmental Research Papers No. 46, Air Force Cambridge Research Laboratories, Hanscom Field, Mass. (1964).
6. McCormick, R. A., and Kurfis, K. R., "Vertical diffusion of aerosols over a city," *Quart. J. Roy. Meteor. Soc.*, **92**, 392–396 (1966).
7. Hamilton, P. M., "The use of lidar in air pollution studies," *Internat. J. Air & Water Poll.*, **10**, 427–434 (1966a).
8. Viezee, W., and Oblanas, J. W., "Lidar-observed haze layers associated with thermal structure in the lower atmosphere," manuscript accepted for publication in *J. Appl. Meteor.* (1969).
9. Johnson, W. B., "Lidar observations of the diffusion and rise of stack plumes," manuscript accepted for publication in *J. Appl. Meteor.* (1969).
10. Hamilton, P. M., "Observations of power station plumes using a pulsed ruby laser rangefinder," *Nature*, **210**, 723–724 (1966b).
11. Hamilton, P. M., "Plume height measurements at Northfleet and Tilbury power stations," *Atmos. Environ.*, **1**, 379–387 (1967).
12. Collis, R. T. H., "Lidar observations of atmospheric motion in forest valleys," *Bull. Amer. Meteor. Soc.*, **49**, 918-922 (1968).
13. Oblanas, J. W., and Collis, R. T. H., "Lidar observations of the Pre-Gondola I test series," Contract No. AT(04-3)-115, Final Report, Proj. 6268, Stanford Res. Inst., Menlo Park, Calif. (1967).
14. Low, M. J. D., "Subtler infrared spectroscopy," *Internat. Sci. and Tech.*, No. **62**, 52–58 (1967).

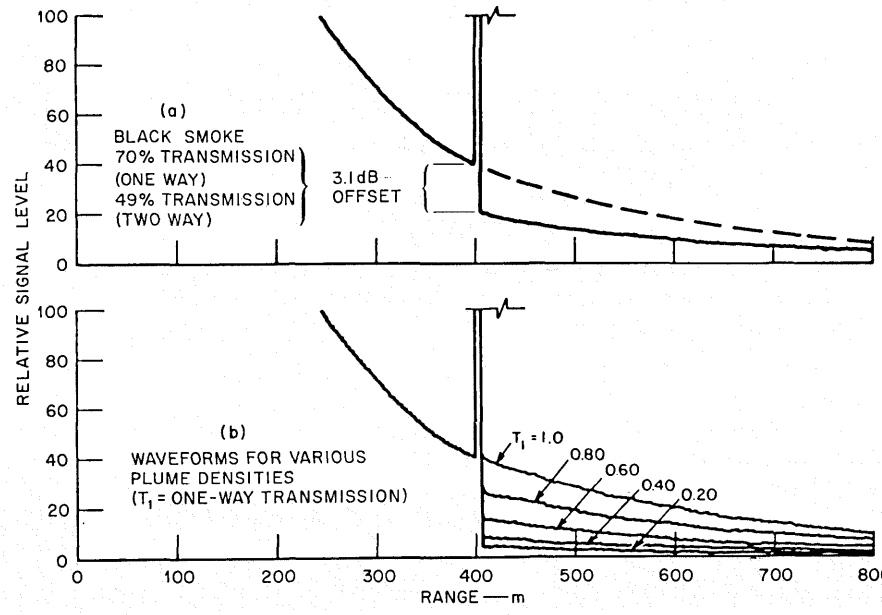

Figure 6. Schematic illustration of technique for obtaining smoke-plume opacity from lidar returns.

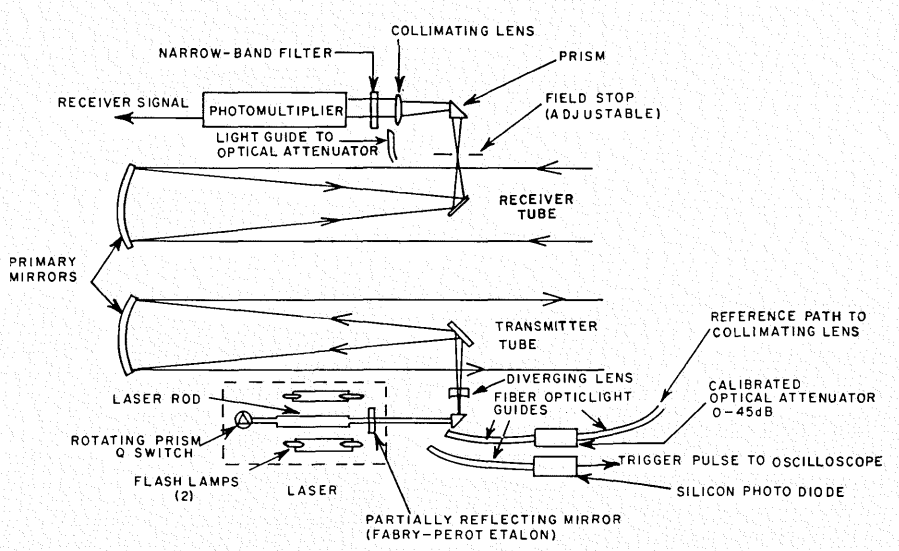

Figure 7. Optical system of the Mark V lidar.

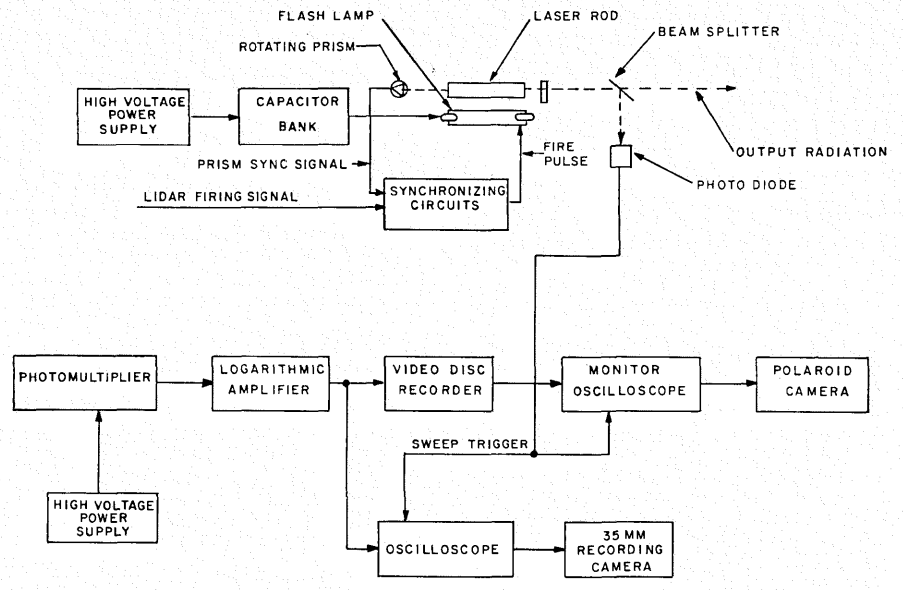

Figure 8. Electronics system of the Mark V lidar.

APPENDIX

Description of Mark V Lidar

The optical system of the Mark V lidar is illustrated in Figure 7. The transmitter consists of a Q-switched, air-cooled, pulsed ruby laser whose output radiation occurs in the deep red portion of the visible spectrum at a wave length of 6943 A. Since the angular resolution of the lidar is determined by the transmitted beam divergence, collimating optics are used to reduce the laser beam divergence and to produce an output beamwidth of 0.35 mrad. The corresponding spatial resolution of this beam is 0.50 m at a range of 1 km in the cross-beam direction, and about 2.3 m in range. The laser cavity is designed to permit the substitution of a neodymium-doped glass laser rod for the ruby rod normally used. The output radiation of the neodymium lidar occurs in the near infrared at a wavelength of 10,600 A. The pulse repetition rate of the Mark V lidar is primarily limited by the capacitor bank charging rate and the cooling rate of the laser cavity. At present, the maximum firing rate is one pulse per 10 seconds for the ruby laser, and one pulse per 5 seconds for the neodymium.

The ruby lidar receiver consists of a 6-inch-diameter Newtonian telescope, identical to the transmitter optics. An adjustable field stop at the focal plane limits the receiver field of view to a maximum of 6 mrad. A multilayered narrowband filter with a wavelength interval (bandwidth) of 13 A is inserted in the receiver optical path to reduce the output noise level produced by solar radiation scattered into the receiver field of view. The detector consists of an RCA 7265 photomultiplier with S-20 spectral response.

The major electronic components of the lidar and the data-recording system are illustrated in the block diagram shown in Figure 8. A compressed-air-driven turbine rotates the laser Q-switching prism at 500 revolutions per second. Upon receipt of a fire signal, the synchronizing generator triggers the flash lamp in step with a signal from the rotating prism. A capacitor bank charged to 3 kv supplies energy for the laser flash lamps. A photodiode senses the occurrence of the laser pulse and produces a trigger pulse to start the oscilloscope sweep. The output of the photomultiplier in the lidar receiver is fed to a pulse amplifier having a logarithmic transer function, and then to an oscilloscope. A Polaroid recording camera mounted on the oscilloscope photographs the lidar return signal. Other data-recording options available include the use of an automatic recording 35-mm camera and a magnetic disc video recorder. The latter device furnishes a steady display on the face of the oscilloscope immediately after each shot, as well as a permanent record, and is very useful for real-time monitoring of observations.

Although the pulse-to-pulse variations of ruby laser power output are not unduly severe, the presence of this random variation introduces a corresponding uncertainty in the amplitude of the received signal unless provision for monitoring the transmitter power is made. The Mark V lidar incorporates an optical feedback arrangement, using fiber-optic light guides, that samples the transmitted energy and injects it into the receiver optical path ahead of the narrowband predetection filter (see Figure 7). This arrangement produces a pulse occurring at zero range on the receiver output. The pulse height is proportional to transmitted power. A variable neutral-density filter is inserted in the fiber-optic path to allow adjustment of the pulse height.

The use of a logarithmic video amplifier in the receiver is almost essential in order to compress the wide dynamic range of the detector (typically four or more orders of magnitude) to enable the received signal to be displayed on a single oscilloscope trace without loss of detailed information.